Doubly Bridged *ansa*-Zirconocenes Based on the Norbornadiene Skeleton: A Quantum Mechanical and Molecular Mechanics Study

Luigi Cavallo,*,† Paolo Corradini,† Gaetano Guerra,† and Luigi Resconi‡

Dipartimento di Chimica, Università di Napoli, Via Mezzocannone 4, I-80134, Napoli, Italy, and Montell Polyolefins, G. Natta Research Center, Piazzale G. Donegani 12, I-44100, Ferrara, Italy

Received April 14, 1995⊗

A quantum mechanical study on the feasibility of doubly bridged *ansa*-zirconocenes based on the norbornadiene skeleton is presented. The enantioselectivity for the propene polymerization by these zirconocenes both with C_2 and C_s symmetry has been investigated by molecular mechanics analysis on models of catalytic intermediates corresponding to the monomer coordination step as well as on models of pseudotransition states relative to the possible monomer insertion reaction. According to our analyses, for suitable substitutions of the norbornadiene skeleton, the models are highly enantioselective. This suggests that both isotactic and syndiotactic polyolefins could be prepared by the corresponding catalytic systems.

Introduction

Stereorigid chiral *ansa*-metallocenes are under active investigation as precatalysts for isospecific olefin polymerization,[1] enantioselective hydrogenation,[2] alkene isomerization,[3] and other stereo- and regiospecific transformations.[4] Much effort has been dedicated to the fine tuning of their catalytic properties by modification of the bis(cyclopentadienyl) π-ligand framework.[1,4] Especially in the case of propene polymerization, it has been realized that the rigidity of the metal complex is directly connected with its catalytic performance: reduction of the conformational freedom of the *ansa*-ligand−metal system has been shown to give rise to higher isospecificities and higher molecular weights.[1,5]

A recurring problem inherent with the synthesis of the majority of these chiral metallocenes is their tendency to form both the meso and the racemic stereomers, which stems from the free rotation of the two Cp moieties around their tether[6] (see Scheme 1). The meso isomer, being achiral and thus aspecific, is usually unwanted and must be removed from the mixture of products by fractional crystallization or solvent extraction. Notable exceptions are Collins' procedure to give pure (*rac*-ethylenebis(1-indenyl))zirconium dichloride,[7] Bercaw's *rac*-$Me_2Si(2\text{-}SiMe_3\text{-}4\text{-}CMe_3C_5H_2)_2YH$ dimer,[8] and the ligands devised by Brintzinger[9] and Bosnich[10] which can yield only racemic, C_2-symmetric metallocenes because of the chiral nature of the bridge and the 1-bridged-3,4-disubstituted cyclopentadienyl ligands. None of these compounds, however, seem to have met the strict requirements for an industrial propylene

Scheme 1

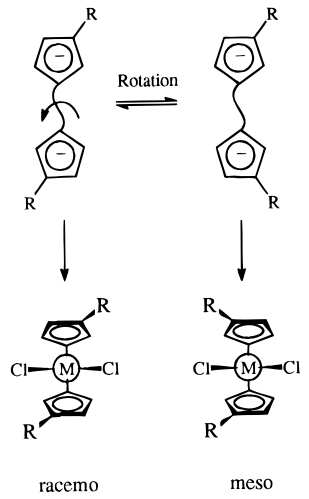

† Università di Napoli. E-mail: cavallo@chemna.dichi.unina.it.
‡ Montell Polyolefins.
⊗ Abstract published in *Advance ACS Abstracts,* March 15, 1996.

(1) See for example: (a) Stehling, U.; Diebold, J.; Kirsten, R.; Röll, W.; Brintzinger, H. H.; Jüngling, S.; Mülhaupt, R.; Langhauser, F. *Organometallics* **1994**, *13*, 964 and references therein. (b) Spaleck, W.; Küber, F.; Winter, A.; Rohrmann, J.; Bachmann, B.; Antberg, M.; Dolle, V.; Paulus, E. *Organometallics* **1994**, *13*, 954 and references therein.

(2) Waymouth, R.; Pino, P. *J. Am. Chem. Soc.* **1990**, *112*, 4911. Willoughby, C.; Buchwald, S. *J. Am. Chem. Soc.* **1992**, *114*, 7562. Willoughby, C.; Buchwald, S. *J. Org. Chem.* **1993**, *58*, 7627. Broene, R.; Buchwald, S. *J. Am. Chem. Soc.* **1993**, *115*, 12569. Lee, N.; Buchwald, S. *J. Am. Chem. Soc.* **1994**, *116*, 5985.

(3) Chen, Z.; Halterman, R. *J. Am. Chem. Soc.* **1992**, *114*, 2276.

(4) Collins, S.; Kuntz, B.; Hong, Y. *J. Org. Chem.* **1989**, *54*, 4154. Grossman, R.; Davis, W.; Buchwald, S. *J. Am. Chem. Soc.* **1991**, *113*, 2321. Hong, Y.; Kuntz, B.; Collins, S. *Organometallics* **1993**, *12*, 964. Morken, J.; Didiuk, M.; Hoveyda, A. *J. Am. Chem. Soc.* **1993**, *115*, 6997. Hoveyda, A.; Morken, J. *J. Org. Chem.* **1993**, *58*, 4237. Halterman, R.; Ramsey, T. *Organometallics* **1993**, *12*, 2879. Halterman, R.; Ramsey, T.; Chen, Z. *J. Org. Chem.* **1994**, *59*, 2642. Rodewald, S.; Jordan, R. *J. Am. Chem. Soc.* **1994**, *116*, 4491.

(5) Herrmann, W.; Rohrmann, J.; Herdtweck, E.; Spaleck, W.; Winter, A. *Angew. Chem., Int. Ed. Engl.* **1989**, *28*, 1511.

(6) Burger, P.; Hortmann, K.; Diebold, J.; Brintzinger, H. H. *J. Organomet. Chem.* **1991**, *417*, 9.

(7) Lee, I.-M.; Gauthier, W.; Ball, J.; Iyengar, B.; Collins, S. *Organometallics* **1992**, *11*, 2115.

(8) Coughlin, E. B.; Bercaw, J. E. *J. Am. Chem. Soc.* **1992**, *114*, 7606.

(9) Huttenloch, M.; Diebold, J.; Rief, U.; Brintzinger, H. H.; Gilbert, A.; Katz, T. *Organometallics* **1992**, *11*, 3600.

(10) Ellis, W.; Hollis, T.; Odenkirk, W.; Whelan, J.; Ostrander, R.; Rheingold, A.; Bosnich, B. *Organometallics* **1993**, *12*, 4391.

S0276-7333(95)00270-6 CCC: $12.00

Chart 1

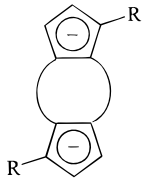

Scheme 2

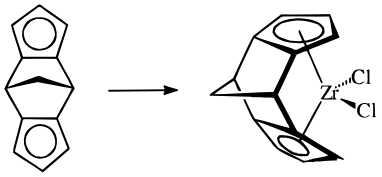

Chart 2

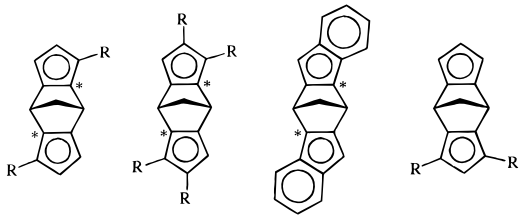

1 2 3 4

R = CH_3, **1a** R = CH_3 R = *t*-Bu

R = Ph, **1b**

R = *t*-Bu, **1c**

Chart 3

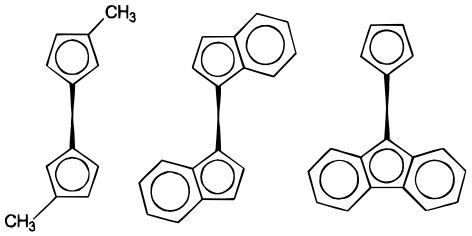

5 6 7

polymerization catalyst, that is, high activity coupled to production of high molecular weight, highly isotactic polymers.

A possible solution to this problem would be to synthesize a C_2-symmetric, properly substituted, stereorigid ligand in its racemic form, that is, a Cp_2 moiety locked in its racemic geometry by virtue of two adjacent bridges, as shown in Chart 1. Vicinal bis(silylene)-bridged bis(cyclopentadienes) have been known for some time, and this approach has been used by Brintzinger to produce some examples of the above class of *ansa*-zirconocenes.[11] However, their polymerization performances are far from satisfying, and a zirconocene structural transformation has been proposed to occur during catalysis, to account for the long induction times observed.

All-carbon doubly bridged ligands are also known;[12] however, their open geometry and lack of proper substitution does not make them the best candidates for the synthesis of the above class of ligands. While this work was in progress, Hafner[13] and Brintzinger[14] reported the synthesis of the first [2](1,1′)[2](2,2′)-zirconocenophane dichloride. This complex, however, has C_{2v} symmetry and lacks the ability of enantioface discrimination for prochiral substrates. A C_2-symmetric, potentially stereoselective version of an all-carbon doubly bridged ligand has been synthesized by Buchwald[15] and used to prepare a chiral titanocene. The Zr and Hf analogues could not be obtained.

We propose here a modification of this class of ligands based on the norbornadiene skeleton (Scheme 2), which was selected for its geometry which is expected to give a limited strain to the final zirconocene derivative, as shown by quantum mechanical calculations. The related C_2 (**1**−**3** of Chart 2) and C_s (**4** of Chart 2) symmetric ligands should give the corresponding C_2 and C_s symmetric metallocenes selectively. Given the potential interest in such metallocenes, we present here some predictions on their enantioface selectivities in propene polymerization based upon our nonbonded interactions analysis.

In the first part of this paper the feasibility of the coordination to the metal atom of the doubly bridged ligands is studied through quantum mechanical calculations. In the second part of this paper, the enantioselectivity and stereospecificity of these catalytic models is evaluated through molecular mechanics calculations relative to diastereoisomeric intermediates preceding the insertion (pre-insertion intermediates) as well as to pseudotransition states for the monomer insertion reaction. For the sake of comparison, analogous molecular mechanics calculations have been performed on model complexes with the similar, single-bridged ligands shown in Chart 3.

Models and Methods

As in previous papers,[16] the models of pre-insertion intermediates and pseudotransition states for the monomer insertion reaction are metal complexes containing three ligands, that is a propene molecule, an isobutyl group (simulating a primary growing chain), and a stereorigid bis(cyclopentadienyl) π-ligand. In this paper several π-ligands, based on the doubly bridged norbornadiene skeleton of Scheme 2, are considered.

A prochiral olefin such as propene may give rise to nonsuperposable coordinations, which can be labeled with the notation *re* and *si*.[17] The coordination of the ligands of kind **1**−**3** of Chart 2 is also chiral and can be labeled with the notation (*R*,*R*) or (*S*,*S*) according to the rules of Cahn−Ingold−Prelog[18] extended to chiral metallocenes as outlined by Schlögl.[19] The symbols (*R*,*R*) and (*S*,*S*) indicate the absolute configuration, for each cyclopentadienyl ring, of the bridgehead

(11) Mengele, W.; Diebold, J.; Troll, C.; Röll, W.; Brintzinger, H. H. *Organometallics* **1993**, *12*, 1931.

(12) Atzkern, H.; Huber, B.; Köhler, F.; Müller, G.; Müller, R. *Organometallics* **1991**, *10*, 238. Dàvila, A.; McLaughlin, M. Presented at the 207th ACS National Meeting, San Diego, CA, March 13−17, 1994; Abstract No. 472.

(13) Hafner, K.; Mink, C.; Lindner, H. J. *Angew. Chem., Int. Ed. Engl.* **1994**, *33*, 1479.

(14) Dorer, B.; Prosenc, M.-H.; Rief, U.; Brintzinger, H.-H. *Organometallics* **1994**, *13*, 3868.

(15) Grossman, R. B.; Tsai, J.-C.; Davis, W. M.; Gutiérrez, A.; Buchwald, S. L. *Organometallics* **1994**, *13*, 3892.

(16) (a) Corradini, P.; Guerra, G.; Vacatello, M.; Villani, V. *Gazz. Chim. Ital.* **1988**, *118*, 173. (b) Cavallo, L.; Guerra, G.; Oliva, L.; Corradini, P.; Vacatello, M. *Polym. Commun.* **1989**, *30*, 16. (c) Cavallo, L.; Corradini, P.; Guerra, G.; Vacatello, M. *Macromolecules* **1991**, *24*, 1784. (d) Cavallo, L.; Corradini, P.; Guerra, G.; Vacatello, M. *Polymer* **1991**, *32*, 1329. (e) Guerra, G.; Cavallo, L.; Moscardi, G.; Vacatello, M.; Corradini, P. *J. Am. Chem. Soc.* **1994**, *116*, 2988. (f) Corradini, P.; Guerra, G. *Prog. Polym. Sci.* **1991**, *16*, 239.

(17) Hanson, K. R. *J. Am. Chem. Soc.* **1966**, *88*, 2731.

carbon atom which is closest to a substituent of the Cp ring (as indicated by a star in Chart 2). Without loss of generality, all the reported calculations, for models with C_2 symmetric ligands, refer to the (*R*,*R*) coordination of the π ligands. For the model complexes with a C_s symmetric ligand, an intrinsic chirality at the central metal atom is present, which, for tetrahedral or assimilable to tetrahedral situations, can be labeled with the notation *R* or *S*, by the extension of the Cahn−Ingold−Prelog rules, as proposed by Stanley and Baird.[20] Without loss of generality, for the C_s symmetric ligands, we only consider the enantiomeric intermediate presenting an *R* chirality at the central metal atom.

The coordination geometries of the stereorigid π ligands **1**−**4** to the Zr atom have been assumed coincident with that calculated for the dichloro complex with the unsubstituted bis-Cp ligand of Scheme 2, by density functional calculations. In any case, considering the lack of reference X-ray structures for a possible check on the reliability of the obtained geometry (and the possible high strain induced in the complex by the double norbornadiene bridge), the geometry was also optimized by the classical *ab-initio* method. The consistency of the geometries obtained by using the two different approaches has been considered essential for the reliability of the molecular mechanics analysis. The coordination geometry of the five-membered rings of the ligands **5**−**7** has been assumed equal to that present in the crystalline structure of Me_2(3-*t*-Bu-C_5H_3)-(3-R-C_9H_5)$ZrCl_2$ reported in ref 21.

Quantum Mechanical Methods. The density functional calculations were carried out by using the HFS-LCAO package ADF, developed by Baerends et al.;[22] the geometry optimization procedure applied for the calculations was based on the method developed by Versluis and Ziegler.[23] The electronic configurations of the systems were described by an uncontracted triple-ζ STO basis set[22] on Zr for 4s, 4p, 4d, 5s, and 5p. Double-ζ STO basis sets[24] were used for C (2s, 2p), H (1s), and Cl (3s, 3p). These basis sets were augmented with single 3d and 2p polarization functions for the C and H atoms, respectively. The $1s^2 2s^2 2p^6 3s^2 3p^6 3d^{10}$ configuration on Zr, the $1s^2$ on C, and $1s^2 2s^2 2p^6$ on Cl were treated by the frozen-core approximation;[22b] a set of auxiliary s, p, d, f, and g STO functions,[25] centered on all nuclei, was used to fit the molecular density. Geometry optimizations were carried out without including nonlocal corrections.

The *ab-initio* calculations were carried out by using the GAMESS package;[26] the geometry optimizations were performed with the restricted Hartree−Fock energy gradient technique. The following basis set has been adopted: For the Zr atom, the effective core potentials (ECP) proposed by Hay and Wadt[27] were used for the core orbitals 1s, 2s, 3s, 2p, 3p, and 3d, with the valence basis functions[27] of split valence contraction (311/311/31), as used by Morokuma in ref 28; for the Cl atoms, the ECP proposed by Hay and Wadt[29] were used for the core orbitals 1s, 2s, and 2p, with the valence basis functions[29] of split valence contractions (21/21); for the C and H atoms, we used the 6-31G basis functions.[30]

Scheme 3

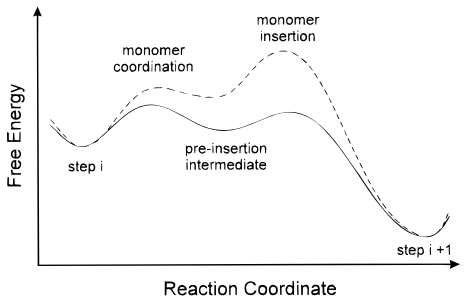

Molecular Mechanics Method. The molecular mechanics analysis has been applied to pre-insertion intermediates, corresponding to the monomer coordination, as well as to pseudotransition states of the monomer insertion reaction. As discussed in detail in a previous report,[31] our molecular mechanics analyses on models for the Ziegler−Natta stereospecific polymerization indicate that the insertion step is the determining one for the enantioselectivity. In fact, large nonbonded energy contributions are calculated for the insertion of the wrong α-olefin enantioface. A schematic plot of the energy versus the reaction coordinate for the propene coordination and insertion with the two possible prochiral faces on a chiral model complex is shown in the Scheme 3. The scheme shows that although, in the framework of our analysis, the insertion step is determining for the enantioselectivity, it should not necessarily be the rate-determining step. Indeed, the energy barrier for the monomer insertion could be small (also null) for the case of ethene as well as for the correct α-olefin enantioface (continuous line in Scheme 3), as predicted by some recent theoretical calculations,[32] while it is certainly high for the wrong α-olefin enantioface (dashed line in Scheme 3).[16a,e]

The calculation method for the nonbonded energy at the catalytic site has been previously described in detail[16e,33] and is not reported here. We only recall the definitions of the most important internal coordinates which have been varied (see Figure 1B): the dihedral angle θ_0 associated with rotations of the olefin around the axis connecting the metal to the center of the double bond and the internal rotation angle θ_1 associated with rotations around the bond between the metal atom and the first carbon atom of the growing chain. At $\theta_0 \approx 0°$ the olefin is oriented in a way suitable for primary insertion, while $\theta_0 \approx 180°$ corresponds to an orientation suitable for secondary insertion. $\theta_1 \approx 0°$ corresponds to the conformation having the first C−C bond of the growing chain eclipsed with respect to the axis connecting the metal atom to the center of the double bond of the olefin.

We also recall that, in the framework of our analysis, alkene-bound intermediates are considered sufficiently close to the transition state, and considered as suitable **pre-insertion intermediates**, only if the insertion can occur through a process of "least nuclear motion".[34] This corresponds to geometries of the alkene-bound intermediates for which (i) the double bond of the olefin is nearly parallel to the bond between the metal atom and the growing chain ($\theta_0 \approx 0°$ or $\theta_0 \approx 180°$)

(18) (a) Cahn, R. S.; Ingold, C.; Prelog, V. *Angew. Chem., Int. Ed. Engl.* **1966**, *5*, 385. (b) Prelog, V.; Helmchem, G. *Angew. Chem., Int. Ed. Engl.* **1982**, *21*, 567.
(19) Schlögl, K. *Top. Stereochem.* **1966**, *1*, 39.
(20) Stanley, K.; Baird, M. C. *J. Am. Chem. Soc.* **1975**, *97*, 6598.
(21) Miyake, S.; Okumura, Y.; Inazawa, S. *Macromolecules* **1995**, *28*, 3074.
(22) Baerends, E. J.; Ellis, D. E.; Ros, P. *Chem. Phys.* **1973**, *2*, 41. (b) Baerends, E. J. Ph.D. Thesis, Vrije Universiteit, Amsterdam, The Netherlands, 1975.
(23) Versluis, L.; Ziegler, T. H. *Chem. Phys.* **1988**, *88*, 322.
(24) Snijders, G. J.; Baerends, E. J.; Vernooijs, P. *At. Nucl. Data Tabl.* **1982**, *26*, 483.
(25) Krijn, J.; Baerends, E. J. *Fit functions in the HFS-method*; Vrije Universiteit: Amsterdam, The Netherlands, 1981.
(26) Schmidt, M. W.; Baldridge, K. K.; Boatz, J. A.; Jensen, J. H.; Koseki, S.; Gordon, M. S.; Nguyen K. A.; Windus, T. L.; Elbert, S. T. *QCPE Bull.* **1990**, *10*, 52.
(27) Hay, P. J.; Wadt, W. R. *J. Chem. Phys.* **1985**, *82*, 299.
(28) Kawamura-Kuribayashi, H.; Koga, N.; Morokuma, K. *J. Am. Chem. Soc.* **1992**, *114*, 8687.
(29) Hay, P. J.; Wadt, W. R. *J. Chem. Phys.* **1985**, *82*, 284.
(30) (a) Ditchfield, R.; Hehre, W. J.; Pople, J. A. *J. Chem. Phys.* **1971**, *54*, 724. (b) Hehre, W. J.; Ditchfield, R.; Pople, J. A. *J. Chem. Phys.* **1972**, *56*, 2257.
(31) Corradini, P.; Barone, V.; Fusco, R.; Guerra, G. *Gazz. Chim. Ital.* **1983**, *113*, 601.
(32) (a) Meier, R. J.; Dormaele, G. H. J.; Iarlori, S.; Buda, F. *J. Am. Chem. Soc.* **1994**, *116*, 7274. (b) Weiss, H.; Ehrig, M.; Ahlrichs, R. H. *J. Am. Chem. Soc.* **1994**, *116*, 4919. (c) Woo, T. K.; Fan, L.; Ziegler, T. *Organometallics* **1994**, *13*, 432. (d) Woo, T. K.; Fan, L.; Ziegler, T. *Organometallics* **1994**, *13*, 2252.
(33) Ammendola, P.; Guerra, G.; Villani, V. *Makromol. Chem.* **1984**, *185*, 2599.

and (ii) the first C−C bond of the chain is nearly perpendicular to the plane defined by the double bond of the monomer and by the metal atom ($|\theta_1| \approx 90°$ rather than $|\theta_1| \approx 180°$). Let us recall that θ_1 values away from 180° and near to 60° are also suited for the formation of an α-agostic bond, which has been shown to stabilize the transition state for the insertion step in some scandium and zirconium-based catalysts.[35] Moreover, alkene-bound intermediates for which the methyl group of the propene and the second carbon atom (and its substituents) of the growing chain are on the same side with respect to the plane defined by the Mt−C bonds ($\theta_1 \approx +60$ and $-60°$ for the *re*- and *si*-coordinated monomers, respectively) are assumed to be unsuitable for the successive monomer insertion. In fact, the insertion paths starting from these intermediates involve large nonbonded interactions.[16,36]

In summary, for the pre-insertion intermediates, the energy differences between the minima observed for $\theta_0 \approx 0°$ at $\theta_1 \approx +60°$ for *si*-propene (E_{si}) and at $\theta_1 \approx -60°$ for *re*-propene (E_{re}) are taken as an approximation to the energy differences which determine the enantioselectivity. It is worth noting that this kind of evaluation of the enantioselectivity for the pre-insertion intermediate is different from that one used by other authors.[37] In those papers, the energy differences between diastereoisomeric intermediates are evaluated by minimizing the energy in the whole range of θ_1. In our computations the minimizations consider only situations suitable for the monomer insertion, and hence, the minimizations with respect to θ_1 are chosen to be only local. This accounts for the much smaller enantioselectivities calculated by other authors.

As for the molecular mechanics analysis of the pre-insertion intermediates, the Zr−C(chain) distance has been assumed equal to 2.28 Å, which is an average of the values observed in cationic zirconocene complexes.[38] Since crystalline structures of d^0 metal−olefin complexes, like those invoked as Ziegler−Natta catalytic intermediates, are not available, it is difficult to assume a reliable distance Zr−C(olefin), which is however expected to be in the range 2.3−2.5 Å.[16e] In this paper, for the sake of simplicity, the distance Zr−C(olefin) has been generally set to a short value (2.3 Å), for which higher values of the enantioselectivity are expected. Test calculations have been repeated by assuming this distance equal to 2.5 Å, obtaining qualitatively similar results.

Although the energy optimizations for the pre-insertion intermediates are more complete than in previous work, we still believe that the numerical results of our calculations cannot be trusted as such. This is especially true for conformations far from the energy minima, because of the unreliability of the energy functions in such regions and because of the simplifying assumption of constancy (rather than near-constancy) of several internal coordinates. However, we also believe that the trends suggested by our results are realistic, in the sense that conformations having low energy according to our calculations are not likely to be substantially different from the energy minima of the catalytic system. Furthermore, although the numerical values of the energy differences depend on the exact geometry and on the energy parameters adopted in the calculations, no reasonable adjustment of these parameters seems to be able to modify our conclusions. As the results of our previous calculations[16] on similar active center models are in a qualitative or, perhaps, semiquantitative agreement with all the available experimental findings, we also believe that such calculations can be used in a predictive way. This is what we attempt to do in the present paper, on systems for which no experimental results of any kind are presently available.

As for the molecular mechanics analysis of the pseudo-transition states, the geometry of the olefin and of the first carbon atom of the growing chain has been set equal to that determined by Ziegler[32c] for the insertion reaction $[Cp_2Zr-CH_3]^+ + CH_2{=}CH_2 \rightarrow [Cp_2Zr-CH_2CH_2CH_3]^+$. In the following calculations, on the basis of the geometry of the transition state for the ethylene insertion, as determined by Ziegler, the value of θ_1 is kept fixed to $-83°$ and to $+83°$, for the *re* and *si* coordination of propene, respectively. While the relative positions of the atoms involved in breaking and forming of bonds are not varied in the calculations, all the other degrees of freedom, already considered at the pre-insertion intermediates, are retained.

The molecular mechanics studies on these pseudo-transition states, with respect to those on pre-insertion intermediates, make the simplifying assumption of constancy of a larger number of internal coordinates. As a consequence, the overestimation of the energies, which is generally expected for the molecular mechanics calculations, is expected to be substantial for this peculiar approach, especially for the doubly bridged *ansa*-zirconocene models.

Results and Discussion

Quantum Mechanical Calculations Relative to the Coordination of the π-Ligand. For the geometry optimizations of the precursor *ansa*-zirconocene dichloride complex of Figure 1A, a C_{2v} symmetry has been imposed; the main geometrical features of this complex are reported in Table 1. The values assumed by the distance Zr−Cn (centroid of the five-membered rings) is 2.14 Å at the density functional level and 2.23 Å at the *ab-initio* level and has to be compared with the value of 2.24 ± 0.02 Å, which represents the experimental mean value observed for the analogous distance in various crystalline compounds.[39] The average C−C bond length in the five-membered rings is 1.41 Å at the density functional level and 1.42 Å at the *ab-initio* level, in good agreement with the experimental mean value (1.40 ± 0.03 Å) observed for the analogous bond length in five-membered rings coordinated to transition metal atoms.[39] The bond distances of the coordinated C atoms from the Zr atom show the usual pattern found in bridged Zr metallocene complexes,[40] i.e., short for the C atoms closer to the bridge (2.41 and 2.47 Å for C2),

(34) (a) Cossee, P. *Tetrahedron Lett.* **1960**, *17*, 12; **1960**, *17*, 17; *J. Catal.* **1964**, *3*, 80; **1964**, *3*, 99. (b) Cossee, P. *The Stereochemistry of Macromolecules*; Ketley, A. D., Ed.; Marcel Dekker: New York, 1967; Vol. 1, Chapter 3. (c) Hine, J. *J. Org. Chem.* **1966**, *31*, 1236. (d) Hine, J. *Adv. Phys. Org. Chem.* **1977**, *15*, 1. (e) Sinnott, M. L. *Adv. Phys. Org. Chem.* **1988**, *24*, 113. (f) Venditto, V.; Corradini, P.; Guerra, G.; Fusco, R. *Eur. Polym. J.* **1991**, *27*, 45.

(35) (a) Kraudelat, H.; Brintzinger, H. H.; *Angew. Chem., Int. Ed. Engl.* **1990**, *29*, 1412. (b) Piers, W. E.; Bercaw, J. E. *J. Am. Chem. Soc.* **1990**, *112*, 9406. (c) Clawson, L.; Soto, J.; Buchwald, S. L.; Steigerwald, M. L.; Grubbs, R. H. *J. Am. Chem. Soc.* **1985**, *107*, 3377.

(36) (a) Corradini, P.; Barone, V.; Fusco, R.; Guerra, G. *Eur. Polym. J.* **1979**, *15*, 133. (b) Corradini, P.; Barone, V.; Fusco, R.; Guerra, G. *J. Catal.* **1982**, *77*, 32. (c) Corradini, P.; Barone, V.; Guerra, G. *Macromolecules* **1982**, *15*, 1242. (d) Corradini, P.; Guerra, G.; Villani, V. *Macromolecules* **1985**, *18*, 1401.

(37) (a) Kawamura-Kuribayashi, H.; Koga, N.; Morokuma, K. *J. Am. Chem. Soc.* **1992**, *114*, 8687. (b) Castonguay, L. A.; Rappé, A. K. *J. Am. Chem. Soc.* **1992**, *114*, 5832. (c) Hart, J. R.; Rappé, A. K. *J. Am. Chem. Soc.* **1993**, *115*, 6159.

(38) (a) Jordan, R.; Bajgur, C.; Willet, R.; Scott, B. *J. Am. Chem. Soc.* **1986**, *108*, 7410. (b) Hlatky, G.; Turner, H.; Eckman, R. *J. Am. Chem. Soc.* **1989**, *111*, 2728. (c) Amorose, D. M.; Lee, R. A.; Petersen, J. L. *Organometallics* **1991**, *10*, 2191. (d) Horton, A.; Orpen, G. A. *Organometallics* **1991**, *10*, 3910. (e) Jordan, R. F.; LaPointe, R. E.; Bradley, P. K.; Baezinger, N. C. *Organometallics* **1989**, *8*, 2892. (f) Jordan, R. F.; Taylor, D. F.; Baezinger, N. C. *Organometallics* **1990**, *9*, 1546. (g) Jordan, R. F.; Taylor, D. F.; Baezinger, N. C. *Organometallics* **1987**, *6*, 1041. (h) Jordan, R. F.; Bradley, P. K.; Baezinger, N. C. *J. Am. Chem. Soc.* **1990**, *112*, 1289.

(39) Orpen, A. G.; Brammer, L.; Allen, F. H.; Kennard, O.; Watson, D. G.; Taylor, R. *J. Chem. Soc., Dalton Trans.* **1989**, *S1*.

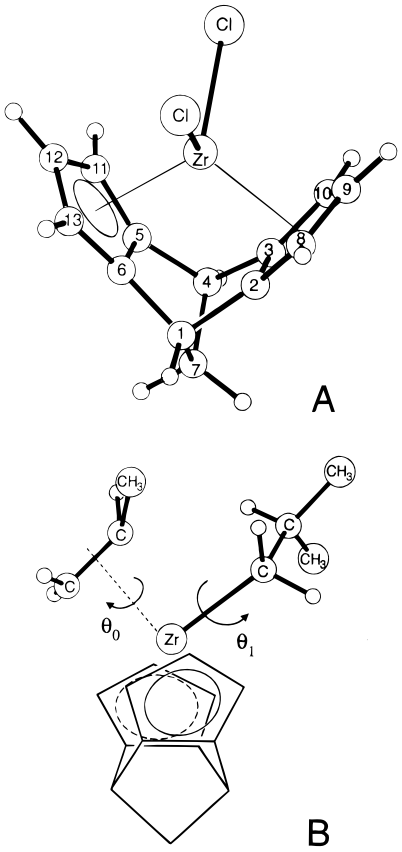

Figure 1. (A) Optimized density functional geometry of the *ansa*-zirconocene dichloro complex including the doubly bridged ligand of Scheme 2, based on the norbornadiene skeleton. The corresponding geometrical parameters are listed in Table 1. (B) Model of pre-insertion intermediate used in the molecular mechanics analysis. The chlorine atoms of model A are substituted by a π-coordinated propene molecule and a σ-coordinated isobutyl (simulating a primary growing chain). The dihedral angles θ_0 and θ_1 are also indicated. For clarity, only the C−C bonds are sketched for the π-ligands. The depicted conformation corresponds to $\theta_0 = 0°$ and $\theta_1 = -60°$.

Table 1. Selected Bond Distances (Å) and Valence Angles (deg) for the *ansa*-Zirconocene Dichloride Complex of Figure 1A

	density functional	*ab initio*		density functional	*ab initio*
Zr−Cl	2.43	2.51	Zr−Cn[a]	2.14	2.23
Zr−C2	2.41	2.47	Zr−C8	2.47	2.57
Zr−C9	2.52	2.60	C2−C3	1.42	1.42
C2−C8	1.41	1.41	C8−C9	1.42	1.43
C1−C2	1.52	1.54	C1−C7	1.54	1.56
Cl−Zr−Cl	108.2	104.2	Cn[a]−Zr−Cn[a]	110.0	108.2
C2−C1−C6	100.6	100.8	C1−C7−C4	96.7	96.5

[a] Cn denotes the centroids of the cyclopentadienyl groups.

intermediate (2.47 and 2.57 Å for C8), and long (2.52 and 2.60 Å for C9), at the density functional and *ab-initio* levels, respectively, which can be compared with the following patterns: 2.42, 2.47−2.50, and 2.56−2.59 Å, found in the crystal structure of (ethylenebis(4,5,6,7-tetrahydro-1-indenyl))$ZrCl_2$;[40a] 2.47−2.49, 2.56−2.59, and 2.66 Å for the crystal structure of (ethylenebis(3-methyl-1-indenyl))$ZrCl_2$;[40c] 2.46, 2.55−2.57, and 2.69−2.67 Å for the fluorenyl ligand in the crystal structure of isopropylidene(1-cyclopentadienyl)(9-fluorenyl)$ZrCl_2$.[40c] Considering that in all the aforementioned complexes, the five-membered ring is considered to be pentahapto coordinated, the same conclusion can be drawn for the structure presented here.

As for the norbornadiene-based bridge, all the calculated geometrical parameters of the coordinated ligand are close to those experimentally observed for the norbornadiene molecule coordinated to a metal atom.[41] It is worth noting that the main geometrical deformation which occurs in norbornadiene upon coordination is relative to the C2−C1−C6 angle, which in the isolated molecule is equal to 107°,[42] while in metal complexes is close to 100°.[41] This angle in the calculated model complex of Figure 1A is equal to 100.6 and 100.8°, at the density functional and *ab-initio* levels, respectively.

All the above discussion indicates that the coordination to the metal atom of the doubly bridged ligands (Schemes 2 and Chart 2) is not strained to any great degree, suggesting the feasibility of these complexes. The substantial agreement between the results obtained by using the two different quantum mechanical approaches considered here makes us confident of the geometry of coordination of the π-ligand, in the following molecular mechanics calculations.

Molecular Mechanics Analysis of the Catalytic Intermediates. The mechanism for the Ziegler−Natta polymerization of the olefins, proposed by Cossee[34a,b] some years ago, assumes that, in the insertion reaction, there is a migration of the growing chain to the position previously occupied by the coordinated monomer (**chain migratory insertion**).

In the framework of this mechanism, the stereospecific behavior of the model sites depends on the relationship between the two pre-insertion intermediates (which in this framework correspond to two successive insertion steps) obtained by exchanging the relative positions of the growing chain and of the incoming monomer. For model sites presenting a C_2 symmetry axis, which locally relates the atoms of the stereorigid π-ligand,[16a,37a] these two pre-insertion intermediates can be identical; i.e., the two available coordination positions are homotopic.[43] These model sites, if the insertion step is enantioselective, are consequently isospecific. For model sites presenting a C_s symmetry plane relating the atoms of the stereorigid π-ligand,[16c,44] these two pre-insertion intermediates can be enantiomeric; i.e., the two available coordination positions are enantiotopic.[43] These model sites, if the insertion step is enantioselective, are consequently syndiospecific. As a consequence, in the following discussion we confine our analysis to the enantioselectivity of a given insertion step.

***C_2* Symmetric Ligands.** Figure 2A−C plots, as a function of θ_1, the optimized energy for the catalytic site models with the π-ligands **1a**−**c** of Chart 2 (with (*R*,*R*) chirality of coordination). Analogously, the Figure 3A,B plots, as a function of θ_1, the optimized energy for the

(40) (a) Ewen, J. A.; Elder, M. J.; Jones, R. L.; Haspeslagh, L.; Atwood, J. L.; Batt, S. G.; Robinson, K. *Makromol. Chem. Symp.* **1991**, *48/49*, 253. (b) Ewen, J. A.; Elder, M. J.; Jones, R. L.; Curtis, S.; Cheng, H. N. In *Catalytic Olefin Polymerization*; Keii, T., Soga, K., Eds.; Elsevier: New York, 1990; p 439. (c) Wild, F. R. W. P.; Zsolnai, L.; Huttner, G.; Brintzinger, H. H. *J. Organomet. Chem.* **1985**, *288*, 63.

(41) Cotton, F. A.; Meadows, J. H. *Inorg. Chem.* **1984**, *23*, 4688.
(42) Burnell, E. E.; Diehl, P. *Can. J. Chem.* **1972**, *50*, 3566.
(43) Mislow, K.; Raban, M. *Top. Stereochem.* **1967**, *1*, 1.
(44) Ewen, J. A.; Jones, R. L.; Razavi, A.; Ferrara, J. D. *J. Am. Chem. Soc.* **1988**, *110*, 6255.

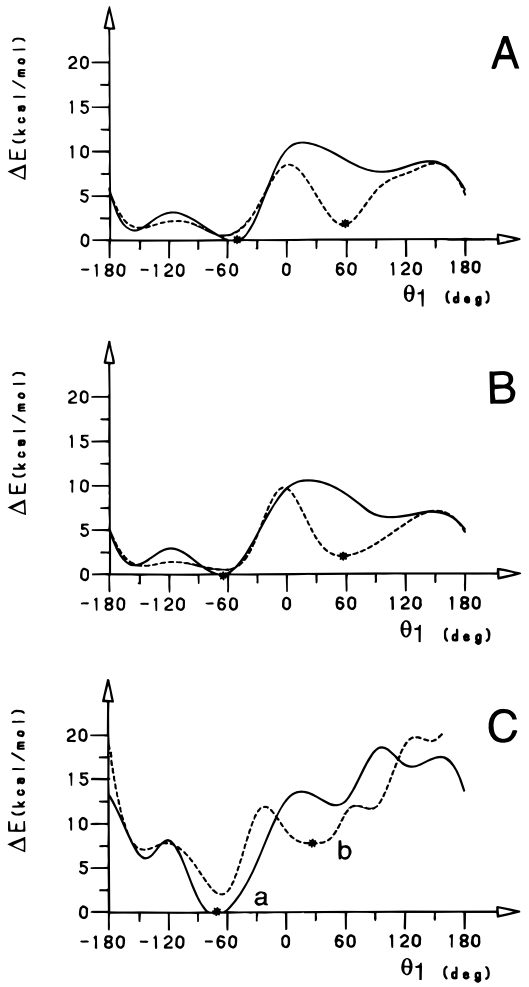

Figure 2. Optimized energies as a function of θ_1, with $\theta_0 \approx 0°$ (see text), for models of pre-insertion intermediates, with (*R*,*R*) chirality of pre-insertion of the C_2 symmetric π-ligands **1**. Parts A−C correspond to models **1a**−**c**, respectively. The full and dashed lines refer to *re*- and *si*-coordinated propene, respectively. The starred minima correspond to pre-insertion intermediates suitable for the primary insertion of propene. The pre-insertion intermediates corresponding to the energy minima labeled with **a** and **b** in (C) are sketched in Figure 4. The energy differences between the starred conformations correspond to the $E_{si} - E_{re}$ values of Table 2.

catalytic site models with the π-ligands **2** and **3** of Chart 2 (always with (*R*,*R*) chirality of coordination), respectively.

The starting points for the energy optimizations in Figures 2 and 3 were the conformations with $\theta_0 = 0°$; whatever the energy, the absolute value of θ_0 for the optimized conformations is not higher than 20°. Hence, these models simulate situations suitable for the primary insertion of propene into a primary polypropylene growing chain. The full and dashed lines refer to *re*- and *si*-coordinated propene, respectively.

The plots of Figure 2 indicate that, in the framework of our analysis, the model with ligand **1** is substantially enantioselective only when the *tert*-butyl substituents are present ($E_{si} - E_{re} \approx 8$ kcal/mol, compare the starred minima in Figure 2C). The calculated energy curves of Figure 3 are qualitatively analogous to those of Figure 2, and the calculated enantioselectivity ($E_{si} - E_{re}$) is slightly lower than 3 kcal/mol for the ligand **2** (Figure 3A) and slightly higher than 4 kcal/mol for the ligand **3**

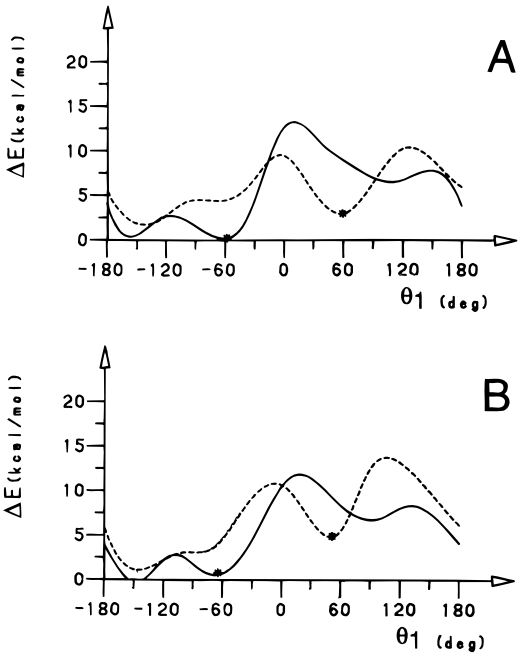

Figure 3. Optimized energies as a function of θ_1, with $\theta_0 \approx 0°$ (see text), for models of pre-insertion intermediates, with (*R*,*R*) chirality of coordination, of the C_2 symmetric π-ligands. Parts A and B correspond to models **2** and **3**, respectively. The full and dashed lines refer to *re*- and *si*-coordinated propene, respectively. The starred minima correspond to pre-insertion intermediates suitable for the primary insertion of propene. The energy differences between the starred conformations correspond to the $E_{si} - E_{re}$ values of Table 2.

(Figure 3B), that is, intermediates between those of Figure 2A,B and that of Figure 2C.

As in models of other *ansa*-metallocenes catalytic complexes,[16] the enantioselectivity is not due to direct interactions of the π-ligands with the monomer but to interactions of the π-ligands with the growing chain, determining its chiral orientation ($\theta_1 \approx -60°$ preferred to $\theta_1 \approx +60°$) which, in turn, discriminates between the two prochiral faces of the propene monomer.

Models corresponding to the minimum energy situations labeled with the letters **a** and **b** in Figure 2C are sketched in Figure 4A,B, respectively. For these models the insertion can occur through a process of "least nuclear motion" (in fact $\theta_0 \approx 0°$ and $|\theta_1| \approx 60°$); moreover for both models, the interactions between the growing chain (at $\theta_1 \approx -60°$ and at $\theta_1 \approx +60°$) and the methyl of the propene monomer (*re*- and *si*-coordinated, respectively) are minimized. Therefore, as discussed in previous papers, for homogeneous[16] as well as for heterogeneous[36] model catalytic intermediates, the models of Figure 4 are both assumed to be suitable for the successive insertion reaction. However, the model with *si* monomer coordination (Figure 4B) is strongly disfavored by repulsive interactions of the growing chain at $\theta_1 \approx +60°$ with one of the *tert*-butyl groups. The other situation with *si* monomer coordination, but with $\theta_1 \approx -60°$ (Figure 2C), is higher in energy (2−3 kcal/mol) with respect to the model with *re* monomer coordination. However, since the methyl group of the propene and the second carbon atom (and its substituents) of the growing chain are on the same side with respect to the plane defined by the Zr−C(olefin) bonds, this situation is

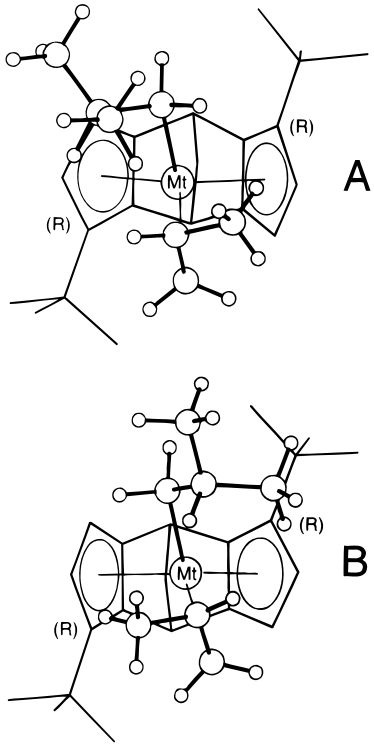

Figure 4. Pre-insertion intermediates for the primary insertion of propene into a primary polypropylene growing chain, when the π-ligand is **1c**. (A) and (B) correspond to the minimum energy situations labeled with the letters **a** and **b** in Figure 2C (for the *re* and *si* monomer coordinations, respectively). The monomer insertion corresponding to the pre-insertion intermediate A, with *re*-propene coordination, is largely favored. The catalytic model site is hence isospecific (see text). For clarity, only the C−C bonds are sketched for the π-ligands.

assumed to be not suitable for the successive monomer insertion.[16,36]

***C_s* Symmetric Ligands.** As cited before, for these model complexes the two intermediates corresponding to two successive insertion steps, in the framework of the chain migratory insertion mechanism, are enantiomorphous. Without loss of generality we consider only the models with the *R* chirality at the central metal atom.

Figure 5 plots, as a function of θ_1, the optimized energy for the catalytic site model with the π-ligand **4**. As for the plots of Figures 2 and 3, the models simulate situations suitable for the primary insertion of propene and the full and dashed lines refer to *re*- and *si*-coordinated propene, respectively. The calculated energy curves of Figure 5 are analogous to those (Figure 2C) of the corresponding model with C_2 symmetry (Figure 4). However, the calculated enantioselectivity is much lower for the syndiospecific with respect to the isospecific model (2 versus 8 kcal/mol).

Models corresponding to the minimum energy situations labeled with the letters **a** and **b** in Figure 5 are sketched in Figure 6A,B, respectively. As can be easily seen in Figure 6A, steric interactions between the methyl group of the coordinated propene and one of the *tert*-butyl groups are present in the conformation of lowest energy, which are instead absent in the corresponding isospecific model (Figure 4A). In the model sketched in Figure 4A, of C_2 symmetry, both the chain and the methyl group of the coordinated propene are located far from the alkyl groups of the ligand. On the other hand, in the model sketched in Figure 4B, both the chain and the methyl group of the coordinated propene are in close contact with the alkyl groups of the ligand. This accounts for the considerable energy difference between the two minima of Figure 4.

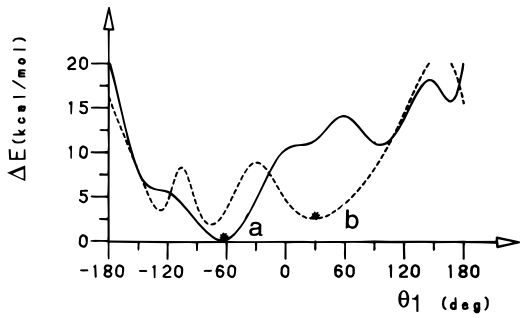

Figure 5. Optimized energies as a function of θ_1, with $\theta_0 \approx 0°$ (see text), for models of pre-insertion intermediates, with *R* chirality at the central metal atom, of the C_s symmetric π-ligand **4**. The full and dashed lines refer to *re*- and *si*-coordinated propene, respectively. The energy minima labeled with **a** and **b** correspond to the pre-insertion intermediates which are sketched in Figure 6. The energy differences between the starred conformations correspond to the $E_{si} - E_{re}$ values of Table 2.

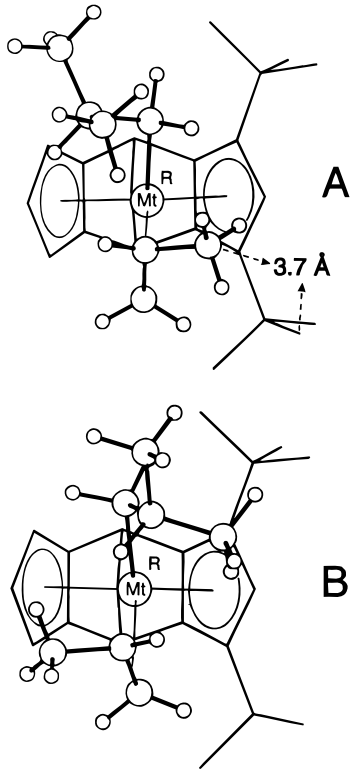

Figure 6. Pre-insertion intermediates for the primary insertion of propene, when the C_s symmetric π-ligand is **3**, with *R* chirality at the central metal atom. (A) and (B) correspond to the minimum energy situations labeled with the letters **a** and **b** in Figure 5A (for the *re* and *si* monomer coordinations, respectively). The monomer insertion corresponding to the pre-insertion intermediate A, with *re* propene coordination, is favored. In the framework of the chain migratory insertion mechanism, the intermediate corresponding to the successive insertion step is the enantiomer of model A (*S* chirality at the central metal atom), which favors *si*-propene coordination and insertion. The catalytic model site is hence syndiospecific.

Table 2. Minimized Energy Differences $E_{si} - E_{re}$ (kcal/mol) for Model Sites Corresponding to the Primary Insertion of Propene into a Primary Polypropene Growing Chain[a]

model, sym	pre-insertion intermediate: Zr−C(olef) = 2.3 Å	pre-insertion intermediate: Zr−C(olef) = 2.5 Å	pseudotransition state
	Double Bridge Models		
1a, C_2	2.3	1.6	3.8
1b, C_2	1.6	1.3	3.0
1c, C_2	7.8	8.5	8.8
2, C_2	2.8	2.8	4.0
3, C_2	4.0	4.0	6.5
4, C_s	2.4	2.2	7.9
	Single Bridge Models		
5, C_2	5.6	5.0	4.8
6, C_2	4.7	3.8	4.7
7, C_s	4.6	4.1	5.1

[a] For the pre-insertion intermediates of models **1a**−**c** and **2**−**4**, the $E_{si} - E_{re}$ values correspond to the energy difference between the starred conformations in Figures 2A−C, 3A,B, and 4, respectively.

In the model sketched in Figure 6A, of C_s symmetry, the chain is far from the alkyl groups of the ligand, while the methyl group of the coordinated propene is on the bulkier side of the ligand. In the model of Figure 6B, the chain is on the bulkier side of the ligand, while the methyl group of the propene is far from the alkyl groups of the ligand. Thus, in both models of Figure 6 there is a steric interaction between the alkyl groups of the ligand and the chain or the propene; this accounts for the relatively small energy difference between the two minima of Figure 6.

As a final point, the dependence of some of our results on the metal−C(olefin) distance is described. Values of $E_{si} - E_{re}$ for the primary insertion of propene into a primary growing chain for the various model sites are reported in Table 2, for the distance metal−C(olefin) set equal to 2.3 and 2.5 Å. It is apparent that the calculated enantioselectivity is scarcely dependent on this distance, as already evidenced for the model site including the bis(ethylene) 1-indenyl ligand.[16e]

Molecular Mechanics Study of Pseudotransition States. The enantioselectivity evaluated on the base of the pre-insertion intermediates is hence lower for the doubly bridged C_s symmetric complex than for the corresponding C_2 symmetric complexes. These calculations could, however, overestimate the reduction of the enantioselectivity in the syndiospecific (C_s symmetric) complexes. In fact, the interaction of the methyl group of the propene with the *tert*-butyl substituents of the π-ligand is, in our opinion, much less relevant in determining the enantioselectivity, with respect to the interaction of the chain with the ligand, because the methyl group of the olefin slips away from the ligand in the course of the insertion reaction.

In order to account for this slipping of the propene toward the growing chain, and in order to have another possible evaluation of the enantioselectivity, we computed the energy difference $E_{si} - E_{re}$ for all of the considered models, using for the olefin and the first carbon atom of the growing chain the geometry of the transition state for the insertion of ethylene into the bond Zr−CH_3, as determined by Ziegler[32c] (see Models and Methods). Let us recall that especially for the doubly bridged models, due to their rigidity, there is an overestimation of the energy differences.

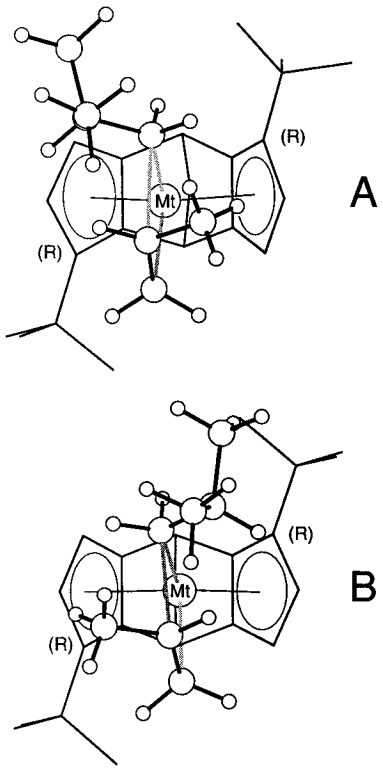

Figure 7. Models of the pseudotransition state for the primary insertion of propene into a primary polypropylene growing chain, when the π-ligand is **1c**, for the *re* and *si* monomer coordinations, respectively. The monomer insertion corresponding to part A, with *re*-propene coordination, is largely favored. The catalytic model site is hence isospecific (see text). For clarity, only the C−C bonds are sketched for the π-ligands, while the bonds which are in the course of formation or breaking are sketched in gray.

***C_2* Symmetric Ligands.** The energy difference $E_{si} - E_{re}$, calculated in this way for the doubly bridged models, is greater with respect to the value obtained for models corresponding to the pre-insertion intermediates (see Table 2); in fact, for all the models of C_2 symmetry, the average increase of the $E_{si} - E_{re}$ value is close to 2.0 kcal/mol.

The models of the pseudotransition state for the insertion of *re*- and *si*-coordinated propene on model **1c** are reported in Figure 7A,B, respectively. By comparison of the models sketched in Figures 4 and 7, it can be desumed that no relevant conformational differences are present between models corresponding to the pre-insertion intermediates and to pseudotransition states.

***C_s* Symmetric Ligands.** As expected, more relevant differences are instead present for models of C_s symmetry. In this case, the energy difference $E_{si} - E_{re}$ grows from 2.4 to 7.9 kcal/mol, thus suggesting a noticeable enantioselective behavior of model **4**.

The models of the pseudotransition state for the insertion of *re*- and *si*-coordinated propene on model **4** are reported in Figure 8A,B, respectively. By comparison of the models sketched in Figures 6 and 8, the origin of the increased enantioselectivity on going from models corresponding to the pre-insertion intermediates to models corresponding to pseudo-transition state can be easily understood. In fact, in the model of Figure 8A, the main steric interaction at the pre-insertion intermediate (see Figure 6A) has been released, being the minimum distance between the C atom of the methyl

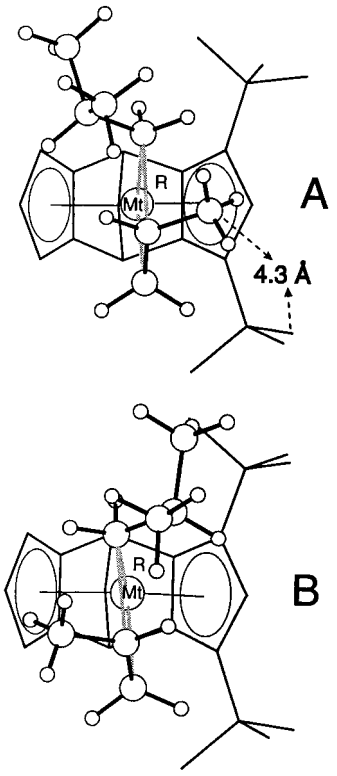

Figure 8. Models of the pseudotransition state for the primary insertion of propene into a primary polypropylene growing chain, when the π-ligand is **4**, for the *re* and *si* monomer coordinations, parts A and B, respectively. The monomer insertion corresponding to part A, with *re*-propene coordination, is largely favored. The catalytic model site is hence syndiospecific (see text). For clarity, only the C−C bonds are sketched for the π-ligands, while the bonds which are in the course of formation or breaking are sketched in gray.

group of the propene, and a C atom of the *tert*-butyl group increased from 3.7 to 4.3 Å. On the other hand, the model of Figure 8B has the growing chain in close contact with one of the *tert*-butyl groups of the ligand.

Molecular Mechanics Analysis of Singly Bridged *ansa*-Zirconocenes. For the sake of comparison, analogous molecular mechanics calculations, relative to diastereoisomeric pre-insertion intermediates as well as pseudo-transition states for the monomer insertion reaction, have been performed for the model complexes with the singly bridged ligands shown in Chart 3. It is well-known that catalytic systems based on ligands **5** and **6** are highly isospecific[5,45,46] and that the catalytic systems based on **7** are highly syndiospecific.[40b] In particular, some experimental values relative to the enantioselectivity, obtained by the dependence of the amount of stereodefects on the polymerization temperature, are available for some isospecific catalytic systems based on **6** (2.9 kcal/mol).[46]

The enantioselectivities of the models with the ligands **5**−**7**, calculated as described in the previous sections for pre-insertion intermediates and for pseudotransition states, are presented in the lower part of Table 2. It is worth noting that, for the models with singly bridged ligands, the differences between the enantioselectivity values obtained by the two different methods are

(45) Mise, T.; Miya, S.; Yamazaki, H. *Chem. Lett.* **1989**, 1853.
(46) Resconi, L. To be published.

Chart 4

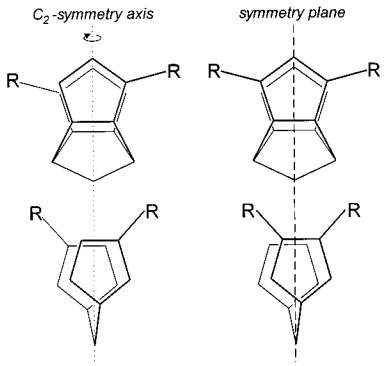

smaller. In fact, the overestimation of the internal energies (and hence of the enantioselectivities) typical of the rigid pseudotransition states of the models with doubly bridged ligands (which include, beside a fixed backbone of the growing chain, relatively rigid π-ligands) is reduced in the presence of more flexible singly bridged ligands. Moreover, the similarity of the enantioselectivities evaluated for the pre-insertion intermediates and pseudotransition states of the C_s symmetric model **7** is due to the substantial absence of direct interactions of the methyl group of the propene with the fluorenyl ligand, as anticipated in ref 16c.

A comparison between the calculated enantioselectivities of Table 2 shows that the models with doubly bridged ligand are less enantioselective with respect to the corresponding singly bridged ligands (e.g., compare model **1a** with model **5** and model **3** with model **6**). This is due to the different orientation of the substituents on the Cp rings. In fact, as shown in Chart 4, the substituents which generate the enantioselectivity, for the case of the doubly bridged ligands, are more distant from the symmetry axis and plane for the case of the C_2 and C_s symmetric ligands, respectively.

Conclusions

The geometry of coordination to a Zr atom of a doubly bridged ligand based on the norbornadiene skeleton and including two cyclopentadienyl (Cp) ligands has been studied, for the case of the dichloro complex, by density functional calculations as well as by a classical *ab-initio* method. The geometries resulting from the two calculation methods are similar and indicate that the two Cp rings can be considered pentahapto coordinated. The coordination to the metal atom of the doubly bridged ligand is not greatly strained; in fact, the calculated geometrical parameters of the coordinated ligand are close to those experimentally observed for the norbornadiene molecule coordinated to a metal atom. These considerations suggest the synthetic feasibility of these complexes.

The geometry of coordination of the unsubstituted doubly bridged π-ligand, calculated by the density functional method, has been used for the molecular mechanics studies on complexes in which the two Cl atoms are substituted by a propene monomer and an isobutyl group (simulating a primary polypropylene growing chain), for different substitutions of the two Cp rings. Molecular mechanics studies have been performed both for the pre-insertion intermediates corresponding to the monomer coordination step as well as

for models of pseudotransition states relative to the possible monomer insertion reaction.

The conclusions from the two sets of molecular mechanics calculations, in the framework of our analysis, if the corresponding catalytic systems are active in the polymerization reaction, are as follows:

(i) For models with a C_2 symmetry of the π-ligand, only the model **1c** (with *tert*-butyl substituents to the two Cp groups) is highly enantioselective (and hence isospecific). Some isospecificity is found also for the model **3** (where the two Cp are substituted by two indenyl ligands), while poor enantioselectivity is found for the models **1a**, **1b**, and **2** (with methyl substituents).

(ii) For the models with a C_s symmetry, a substantial enantioselectivity (and hence syndiospecificity) is found for model **4** (again with *tert*-butyl substituents). The enantioselectivity is however expected to be lower than for the corresponding C_2 symmetric isospecific model **1c**.

(iii) The enantioselectivity of the complexes with the doubly bridged ligands is always lower with respect to that of the complexes with the corresponding single bridged ligands.

Note Added in Proof: A C_s-symmetric ligand with two Me_2Si bridges and two isopropyl substituents on one Cp ring, hence very similar to **4**, has been shown to generate a syndiospecific zirconocene.[47]

Acknowledgment. We thank Prof. Ziegler of the University of Calgary for providing us with the complete set of coordinates of the transition state used in the present work and one of the reviewers for the suggestion of introducing Chart 4. The financial support of the "Progetto Strategico Tecnologie Chimiche Innovative", of the "Ministero dell'Università e della Ricerca Scientifica e Tecnologica" of Italy, and of Montell Polyolefins is also acknowledged.

OM9502704

(47) Bercaw, J. Paper presented at the 211th National Meeting of the American Chemical Society, New Orleans, LA, March 24−28, 1996.